

# Convergence of the Chiral Expansion in Two-Flavor Lattice QCD

著者別名	青木 慎也
journal or publication title	Physical review letters
volume	101
number	20
page range	202004
year	2008-11
権利	(C) 2008 The American Physical Society
URL	<a href="http://hdl.handle.net/2241/101314">http://hdl.handle.net/2241/101314</a>

doi: 10.1103/PhysRevLett.101.202004

## Convergence of the Chiral Expansion in Two-Flavor Lattice QCD

J. Noaki,<sup>1</sup> S. Aoki,<sup>2,3</sup> T. W. Chiu,<sup>4</sup> H. Fukaya,<sup>5,1</sup> S. Hashimoto,<sup>1,6</sup> T. H. Hsieh,<sup>7</sup> T. Kaneko,<sup>1,6</sup> H. Matsufuru,<sup>1</sup> T. Onogi,<sup>8</sup>  
E. Shintani,<sup>1</sup> and N. Yamada<sup>1,6</sup>

(JLQCD and TWQCD Collaborations)

<sup>1</sup>High Energy Accelerator Research Organization (KEK), Tsukuba 305-0801, Japan

<sup>2</sup>Graduate School of Pure and Applied Sciences, University of Tsukuba, Tsukuba 305-8571, Japan

<sup>3</sup>Riken BNL Research Center, Upton, New York 11973, USA

<sup>4</sup>Physics Department, Center for Theoretical Sciences, and National Center for Theoretical Sciences, National Taiwan University, Taipei 10617, Taiwan

<sup>5</sup>The Niels Bohr Institute, The Niels Bohr International Academy, Blegdamsvej 17 DK-2100 Copenhagen Ø Denmark

<sup>6</sup>School of High Energy Accelerator Science, The Graduate University for Advanced Studies (Sokendai), Tsukuba 305-0801, Japan

<sup>7</sup>Research Center for Applied Sciences, Academia Sinica, Taipei 115, Taiwan

<sup>8</sup>Yukawa Institute for Theoretical Physics, Kyoto University, Kyoto 606-8502, Japan

(Received 9 June 2008; published 13 November 2008)

We test the convergence property of the chiral perturbation theory using a lattice QCD calculation of pion mass and decay constant with two dynamical quark flavors. The lattice calculation is performed using the overlap fermion formulation, which realizes exact chiral symmetry at finite lattice spacing. By comparing various expansion prescriptions, we find that the chiral expansion is well saturated at the next-to-leading order for pions lighter than  $\sim 450$  MeV. Better convergence behavior is found, in particular, for a resummed expansion parameter  $\xi$ , with which the lattice data in the pion mass region 290–750 MeV can be fitted well with the next-to-next-to-leading order formulas. We obtain the results in two-flavor QCD for the low energy constants  $\bar{L}_3$  and  $\bar{L}_4$  as well as the pion decay constant, the chiral condensate, and the average up and down quark mass.

DOI: 10.1103/PhysRevLett.101.202004

PACS numbers: 12.38.Gc, 11.15.Ha, 11.30.Rd, 12.39.Fe

Chiral perturbation theory (ChPT) is a powerful tool to analyze the dynamics of low energy pions [1]. The expansion parameter in ChPT is the pion mass (or momentum) divided by the typical scale of the underlying theory such as quantum chromodynamics (QCD). Good convergence of the chiral expansion is observed for physical pions in the analysis including the next-to-next-to-leading order (NNLO) for the pion-pion scattering [2], for instance. In the kaon mass region, on the other hand, the validity of ChPT is not obvious and in fact an important issue in many phenomenological applications.

Lattice QCD calculation can, in principle, be used for a detailed test of the convergence property of ChPT, as one can freely vary the quark mass, typically in the range  $m_s/5 \sim m_s$  with  $m_s$  the physical strange quark mass. However, such a direct test has been difficult, since the lattice regularization of the quark action explicitly violates flavor and/or chiral symmetry in the conventional formulations, such as the Wilson and staggered fermions. One then has to introduce additional terms with unknown parameters to describe those violations in ChPT; hence, the test requires precise continuum extrapolation.

The aim of this article is to provide a direct comparison between the ChPT predictions and lattice QCD calculations, using the overlap fermion formulation on the lattice,

that preserves exact chiral symmetry at finite lattice spacing  $a$  [3,4]. With the exact chiral symmetry, the use of the continuum ChPT is valid to describe the lattice data at a finite lattice spacing up to Lorentz violating corrections; the discretization error of  $\mathcal{O}(a^2)$  affects the value of the low energy constants (LECs) and unknown Lorentz violating corrections. To make a cleaner analysis, we consider two-flavor QCD in this work, leaving the similar study in 2 + 1-flavor QCD, which introduces much more complications, for a future work. We calculate the pion mass and decay constant, for which the NNLO calculations are available in ChPT [5]. A preliminary report of this work is found in [6].

Lattice simulations are performed on a  $L_s^3 \times L_t = 16^3 \times 32$  lattice at a lattice spacing  $a = 0.1184(03) \times (21)$  fm determined with an input  $r_0 = 0.49$  fm, the Sommer scale defined for the heavy quark potential. At six different sea quark masses  $m_{\text{sea}}$ , covering the pion mass region  $290 \text{ MeV} \lesssim m_\pi \lesssim 750 \text{ MeV}$ , we generate 10 000 trajectories, among which the calculation of the pion correlator is carried out at every 20 trajectories. For further details of the simulation we refer [7].

In the calculation of the pion correlator, we computed in advance the lowest 50 conjugate pairs of eigenmode of the overlap-Dirac operator on each gauge configuration and

stored on the disk. Then, by using the eigenmodes to construct a preconditioner, the inversion of the overlap-Dirac operator can be done with only  $\approx 15\%$  of the CPU time of the full calculation. The low modes are also used to improve the statistical accuracy by averaging their contribution to the correlators over 32 source points distributed in each time slice. The correlators are calculated with a point source and a smeared source; the pion mass  $m_\pi$  and decay constant  $f_\pi$  are obtained from a simultaneous fit of them.

The pion decay constant  $f_\pi$  is defined through  $\langle 0 | \mathcal{A}_\mu | \pi(p) \rangle = i f_\pi p_\mu$ , where  $\mathcal{A}_\mu$  is the (continuum) isotriplet axial-vector current. Instead of  $\mathcal{A}_\mu$ , we calculate the matrix element of pseudoscalar density  $P^{\text{lat}}$  on the lattice using the partially-conserved-axial-vector-current constraint relation  $\partial_\mu \mathcal{A}_\mu = 2m_q^{\text{lat}} P^{\text{lat}}$  with  $m_q^{\text{lat}}$  the bare quark mass. Since the combination  $m_q^{\text{lat}} P^{\text{lat}}$  is not renormalized, no renormalization factor is needed in the calculation of  $f_\pi$ . This is possible only when the chiral symmetry is exact. The renormalization factor for the quark mass  $m_q = Z_m^{\overline{\text{MS}}}(2 \text{ GeV}) m_q^{\text{lat}}$  is calculated nonperturbatively through the RI/MOM scheme, with which the renormalization condition is applied at some off-shell momentum for propagators and vertex functions. Such a nonperturbative calculation suffers from the nontrivial quark mass dependence of the chiral condensate. By using the calculated low-modes explicitly, we are able to control the mass dependence to determine  $Z_m^{\text{RI/MOM}}$  more reliably. In the chiral limit, we obtain  $Z_m^{\overline{\text{MS}}}(2 \text{ GeV}) = 0.838(14)(03)$ , where the second error arises from a subtraction of power divergence from the chiral condensate. The details of this calculation will be given elsewhere.

Since our numerical simulation is done on a finite volume lattice with  $m_\pi L_s \approx 2.9$  for the lightest sea quark, the finite volume effect could be significant. We make a correction for the finite volume effect using the estimate within ChPT calculated up to  $\mathcal{O}[m_\pi^4/(4\pi f_\pi)^4]$  [8]. The size of the corrections for  $m_\pi^2$  and  $f_\pi$  is about 5% for the lightest pion mass and exponentially suppressed for heavier data points. In addition, there is a correction due to fixing the global topological charge in our simulation [7,9]. This leads to a finite volume effect of  $\mathcal{O}(1/V)$  with  $V$  the physical space-time volume. The correction is calculable within ChPT [10,11] depending on the value of topological susceptibility  $\chi_t$ , which we calculated in [12]. At next-to-leading order (NLO), the correction for  $m_\pi^2$  is similar in magnitude but opposite in sign to the ordinary finite volume effect at the lightest pion mass, and thus almost cancels. For  $f_\pi$  the finite volume effect due to the fixed topology starts at NLO and therefore is a subdominant effect. Note that the LECs appear in the calculation of these correction factors. We use their phenomenological values at the scale of physical (charged) pion mass  $m_{\pi^+} = 139.6 \text{ MeV}$ :  $\bar{l}_1^{\text{phys}} = -0.4 \pm 0.6$ ,  $\bar{l}_2^{\text{phys}} = 4.3 \pm 0.1$ ,  $\bar{l}_4^{\text{phys}} =$

$4.4 \pm 0.2$ , determined at the NNLO [2] and  $\bar{l}_3^{\text{phys}} = 2.9 \pm 2.4$ . The errors in these values are reflected in the following analysis assuming a Gaussian distribution.

After applying the finite volume corrections, we first analyze the numerical data for  $m_\pi^2/m_q$  and  $f_\pi$  using the ChPT formulas at NLO,

$$m_\pi^2/m_q = 2B(1 + \frac{1}{2}x \ln x) + c_3 x, \quad (1)$$

$$f_\pi = f(1 - x \ln x) + c_4 x, \quad (2)$$

where  $f$  is the pion decay constant in the chiral limit and  $B$  is related to the chiral condensate. Here the expansion is made in terms of  $x \equiv 4Bm_q/(4\pi f)^2$ . The parameters  $c_3$  and  $c_4$  are related to the LECs  $\bar{l}_3^{\text{phys}}$  and  $\bar{l}_4^{\text{phys}}$ , respectively. At NLO, i.e.,  $\mathcal{O}(x)$ , these expressions are unchanged when one replaces the expansion parameter  $x$  by  $\hat{x} \equiv 2m_\pi^2/(4\pi f)^2$  or  $\xi \equiv 2m_\pi^2/(4\pi f_\pi)^2$ , where  $m_\pi$  and  $f_\pi$  denote those at a finite quark mass. Therefore, in a small enough pion mass region the three expansion parameters should describe the lattice data equally well.

Three fit curves ( $x$  fit,  $\hat{x}$  fit, and  $\xi$  fit) for the three lightest pion mass points ( $m_\pi \leq 450 \text{ MeV}$ ) are shown in Fig. 1 as a function of  $m_\pi^2$ . From the plot we observe that the different expansion parameters seem to describe the three lightest points equally well; the values of  $\chi^2/\text{dof}$  are 0.30, 0.33, and 0.66 for  $x$ ,  $\hat{x}$ , and  $\xi$  fits. In each fit, the correlation

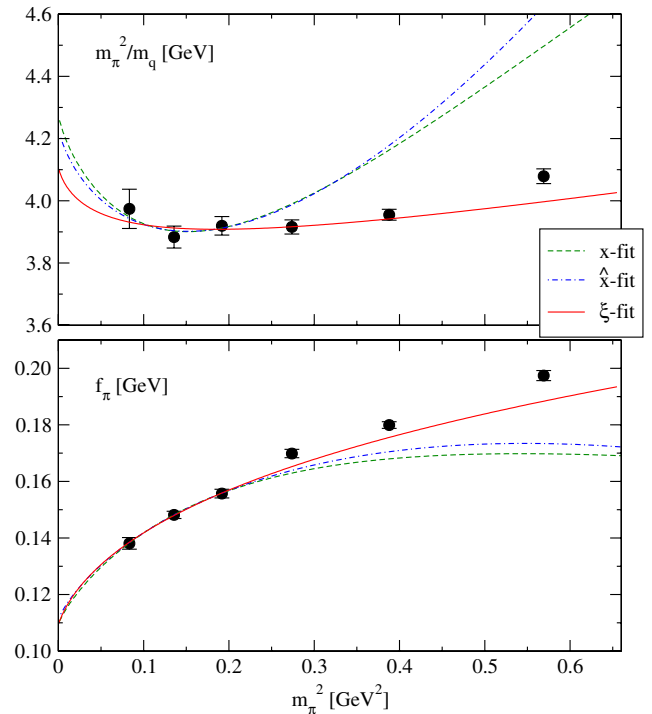


FIG. 1 (color online). Comparison of the chiral fits including the NLO terms for  $m_\pi^2/m_q$  (top) and  $f_\pi$  (bottom). Fit curves to three lightest data points obtained with different choices of the expansion parameter ( $x$ ,  $\hat{x}$ , and  $\xi$ ) are shown as a function of  $m_\pi^2$ .

between  $m_\pi^2/m_q$  and  $f_\pi$  for common sea quark mass is taken into account. Between the  $x$  and  $\hat{x}$  fit, all of the resulting fit parameters are consistent. Among them,  $B$  and  $f$ , the LECs at the leading order ChPT are also consistent with the  $\xi$  fit. This indicates that the NLO formulas successfully describe the data.

The agreement among the different expansion prescriptions is lost (with the deviation greater than  $3\sigma$ ) when we extend the fit range to include the next lightest data point at  $m_\pi \simeq 520$  MeV. We, therefore, conclude that for these quantities the NLO ChPT may be safely applied only below  $\simeq 450$  MeV.

Another important observation from Fig. 1 is that only the  $\xi$  fit reasonably describes the data beyond the fitted region. With the  $x$  and  $\hat{x}$  fits the curvature due to the chiral logarithm is too strong to accommodate the heavier data points. In fact, values of the LECs with the  $x$  and  $\hat{x}$  fits are more sensitive to the fit range than the  $\xi$  fit. This is because  $f$ , which is significantly smaller than  $f_\pi$  of our data, enters in the definition of the expansion parameter. Qualitatively, by replacing  $m_q$  and  $f$  by  $m_\pi^2$  and  $f_\pi$  the higher loop effects in ChPT are effectively resummed and the convergence of the chiral expansion is improved.

We then extend the analysis to include the NNLO terms. Since we found that only the  $\xi$  fit reasonably describes the data beyond  $m_\pi \simeq 450$  MeV, we perform the NNLO analysis using the  $\xi$  expansion in the following. With other expansion parameters, the NNLO fits including heavier mass points are unstable. At the NNLO, the formulas in the  $\xi$  expansion are [2]

$$\begin{aligned} m_\pi^2/m_q = 2B & \left[ 1 + \frac{1}{2} \xi \ln \xi + \frac{7}{8} (\xi \ln \xi)^2 \right. \\ & + \left. \left( \frac{c_4}{f} - \frac{1}{3} (\tilde{l}^{\text{phys}} + 16) \right) \xi^2 \ln \xi \right] \\ & + c_3 \xi \left( 1 - \frac{9}{2} \xi \ln \xi \right) + \alpha \xi^2, \end{aligned} \quad (3)$$

$$\begin{aligned} f_\pi = f & \left[ 1 - \xi \ln \xi + \frac{5}{4} (\xi \ln \xi)^2 + \frac{1}{6} \left( \tilde{l}^{\text{phys}} + \frac{53}{2} \right) \xi^2 \ln \xi \right] \\ & + c_4 \xi (1 - 5 \xi \ln \xi) + \beta \xi^2. \end{aligned} \quad (4)$$

In the terms of  $\xi^2 \ln \xi$ , the LECs at NLO appear:  $\tilde{l}^{\text{phys}} \equiv 7\tilde{l}_1^{\text{phys}} + 8\tilde{l}_2^{\text{phys}} - 15 \ln(2\sqrt{2}\pi f_\pi^{\text{phys}}/m_{\pi^+})^2$ , where  $f_\pi^{\text{phys}} = 130.7$  MeV. We input the phenomenological estimate  $\tilde{l}^{\text{phys}} = -32.0 \pm 4.3$  to the fit. Since the data are not precise enough to discriminate between  $\xi^2 \ln \xi$  and  $\xi^2$  in the given region of  $\xi$  (0.06–0.19), fit parameters  $\alpha$  and  $\beta$  partially absorb the uncertainty in  $\tilde{l}^{\text{phys}}$ . In fact, our final results for the LECs are insensitive to  $\tilde{l}^{\text{phys}}$ .

In Fig. 2, we show the NNLO fits using all the data points (solid curves). In these plots  $m_\pi^2/m_q$  and  $f_\pi$  are normalized by their values in the chiral limit. As expected

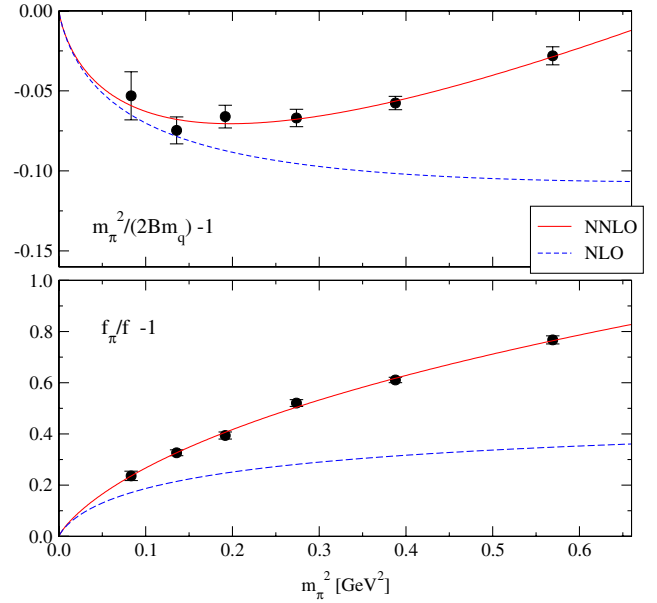


FIG. 2 (color online). NNLO chiral fits using all the data points for  $m_\pi^2/m_q$  (top) and  $f_\pi$  (bottom). Data are normalized by the value in the chiral limit. Solid curves show the NNLO fit, and the truncated expansions at NLO are shown by dashed curves.

from the good convergence of the  $\xi$  fit even at NLO, the NNLO formulas nicely describe the lattice data in the whole data region. We also draw a truncation at the NLO level (dashed curves) but using the same fit parameters. The difference between the NLO truncated curves and the NLO fit curves to the three lightest data points (Fig. 1) is explained by the presence of the terms  $\xi(1 - \frac{9}{2}\xi \ln \xi)$  and  $\xi(1 - 5\xi \ln \xi)$  in (3) and (4), respectively. Since the factors  $(1 - \frac{9}{2}\xi \ln \xi)$  and  $(1 - 5\xi \ln \xi)$  are significantly larger than 1 in the data region, the resulting fit parameters  $c_3$  and  $c_4$  in the NNLO formulas are much lower than those of the NLO fits. This indicates that the determination of the NLO LECs is quite sensitive to whether the NNLO terms are included in the analysis, while the leading order LECs are stable.

From Fig. 2 we can explicitly observe the convergence behavior of the chiral expansion. For instance, at the kaon mass region  $m_\pi \sim 500$  MeV, the NLO term contributes at a  $-10\%$  ( $+28\%$ ) level to  $m_\pi^2/m_q$  ( $f_\pi$ ), and the correction at NNLO is about  $+3\%$  ( $+18\%$ ). At least, the expansion is converging (NNLO is smaller than NLO) for both of these quantities, but quantitatively the convergence behavior depends significantly on the quantity of interest. For  $f_\pi$  the NNLO contribution is already substantial at the kaon mass region.

From the  $\xi$  fit, we extract the LECs of ChPT, i.e., the decay constant in the chiral limit  $f$ , chiral condensate  $\Sigma = Bf^2/2$ , and the NLO LECs  $\tilde{l}_3^{\text{phys}} = -c_3/B + \ln(2\sqrt{2}\pi f/m_{\pi^+})^2$  and  $\tilde{l}_4^{\text{phys}} = c_4/f + \ln(2\sqrt{2}\pi f/m_{\pi^+})^2$ . For each quantity, a comparison of the results between

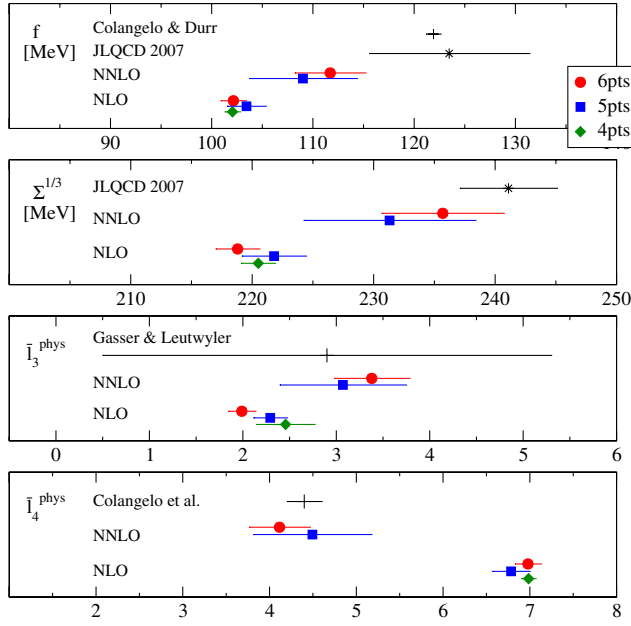


FIG. 3 (color online). Comparison of the ChPT parameters obtained from the NLO fit and NNLO fit. Red circles, blue squares, and green diamonds are corresponding to the results of the fit using the lightest 4, 5, and all 6 data points. Error bars indicate statistical error. Pluses and stars represent reference points.

the NLO and the NNLO fits is shown in Fig. 3. In each panel, the results with 5 and 6 lightest data points are plotted for the NNLO fit. The correlated fits give  $\chi^2/\text{dof} = 1.94$  and  $1.40$ , respectively. For the NLO fits, we plot results obtained with 4, 5, and 6 points to show the stability of the fit. The  $\chi^2/\text{dof}$  is less than  $1.94$ . The results for these physical quantities are consistent within either the NLO or the NNLO fit. On the other hand, as seen for  $\bar{l}_4^{\text{phys}}$  most prominently, there is a significant disagreement between NLO and NNLO. This is due to the large NNLO coefficients as already discussed.

We quote our final results from the NNLO fit with all data points:  $f = 111.7(3.5)(1.0)_{(-0.0)}^{(+6.0)}$  MeV,  $\Sigma^{\overline{\text{MS}}}(2 \text{ GeV}) = [235.7(5.0)(2.0)_{(-0.0)}^{(+12.7)}] \text{MeV}^3$ ,  $\bar{l}_3^{\text{phys}} = 3.38(40)(24)_{(-0)}^{(+31)}$ , and  $\bar{l}_4^{\text{phys}} = 4.12(35)(30)_{(-0)}^{(+31)}$ . From the value at the neutral pion mass  $m_{\pi^0} = 135.0$  MeV, we obtain the average up and down quark mass  $m_{ud}$  and the pion decay constant as  $m_{ud}^{\overline{\text{MS}}}(2 \text{ GeV}) = 4.452(81)(38) \times_{(-227)}^{(+0)}$  MeV and  $f_{\pi} = 119.6(3.0)(1.0)_{(-0.0)}^{(+6.4)}$  MeV. In these results, the first error is statistical, where the error of the renormalization constant is included in quadrature for  $\Sigma^{1/3}$  and  $m_{ud}$ . The second error is systematic due to the truncation of the higher order corrections, which is estimated by an order counting with a coefficient of  $\approx 5$  as appeared at NNLO. For quantities carrying mass dimensions, the third error is from the ambiguity in the determination of  $r_0$ . We

estimate these errors from the difference of the results with our input  $r_0 = 0.49$  fm and that with  $0.465$  fm [13]. The third errors for  $\bar{l}_3^{\text{phys}}$  and  $\bar{l}_4^{\text{phys}}$  reflect an ambiguity of choosing the renormalization scale of ChPT ( $4\pi f$  or  $4\pi f_{\pi}$ ). There are other possible sources of systematic errors that are not reflected in the error budget. They include the discretization effect, remaining finite volume effect, and the effect of missing strange quark in the sea.

In each panel of Fig. 3, we also plot reference points (pluses and stars) for comparison. Overall, with the NNLO fits, we find good agreement with those reference values. For  $f$ , our result is significantly lower than the two-loop result in two-flavor ChPT [14],  $f = 121.9 \pm 0.7$  MeV, but taking account of the scale uncertainty, which is not shown in the plot, the agreement is more reasonable. For  $f$  and  $\Sigma^{\overline{\text{MS}}}(2 \text{ GeV})$ , we also plot the lattice results from our independent simulation in the  $\epsilon$  regime [15]. We observe a good agreement with the NNLO fits. Comparison of the LECs  $\bar{l}_3^{\text{phys}}$  and  $\bar{l}_4^{\text{phys}}$  with the phenomenological values [2] also favor the NNLO fits, especially for  $\bar{l}_4^{\text{phys}}$ .

With the presently available computational power, the chiral extrapolation is still necessary in the lattice QCD calculations. The consistency test of the lattice data with ChPT as described in this Letter is crucial for reliable chiral extrapolation of any physical quantities to be calculated on the lattice. With a two-flavor simulation preserving exact chiral symmetry, we demonstrate that the lattice data are well described by the use of the resummed expansion parameter  $\xi = 2m_{\pi}^2/(4\pi f_{\pi})^2$ . Extension of the analysis to the case of partially quenched QCD [16] and to other physical quantities, such as the pion form factor [17] is ongoing. Also, simulations with exact chiral symmetry including dynamical strange quark are under way [18].

Numerical simulations are performed on Hitachi SR11000 and IBM System Blue Gene Solution at High Energy Accelerator Research Organization (KEK) under a support of its Large Scale Simulation Program (Nos. 07–16). H. F. was supported by Nishina Foundation. This work is supported in part by the Grant-in-Aid of the Ministry of Education (Nos. 17740171, 18034011, 18340075, 18740167, 18840045, 19540286, 19740121, 19740160, 20025010, 20039005, 20340047, 20740156), the National Science Council of Taiwan (Nos. NSC96-2112-M-002-020-MY3, NSC96-2112-M-001-017-MY3), and NTU-CQSE (97R0066-65/69).

- [1] J. Gasser and H. Leutwyler, Ann. Phys. (N.Y.) **158**, 142 (1984).
- [2] G. Colangelo, J. Gasser, and H. Leutwyler, Nucl. Phys. **B603**, 125 (2001).
- [3] H. Neuberger, Phys. Lett. B **417**, 141 (1998).
- [4] H. Neuberger, Phys. Lett. B **427**, 353 (1998).
- [5] J. Bijnens, G. Colangelo, and P. Talavera, J. High Energy Phys. 05 (1998) 014.

- [6] J. Noaki *et al.* (JLQCD Collaboration), Proc. Sci., LAT2007 (2007) 126.
- [7] S. Aoki *et al.* (JLQCD Collaboration), Phys. Rev. D **78**, 014508 (2008).
- [8] G. Colangelo, S. Durr, and C. Haefeli, Nucl. Phys. **B721**, 136 (2005).
- [9] H. Fukaya *et al.* (JLQCD Collaboration), Phys. Rev. D **74**, 094505 (2006).
- [10] R. Brower, S. Chandrasekharan, J. W. Negele, and U. J. Wiese, Phys. Lett. B **560**, 64 (2003).
- [11] S. Aoki, H. Fukaya, S. Hashimoto, and T. Onogi, Phys. Rev. D **76**, 054508 (2007).
- [12] S. Aoki *et al.* (JLQCD and TWQCD Collaborations), Phys. Lett. B **665**, 294 (2008).
- [13] C. Aubin *et al.* (MILC), Phys. Rev. D **70**, 114501 (2004).
- [14] G. Colangelo and S. Durr, Eur. Phys. J. C **33**, 543 (2004).
- [15] H. Fukaya *et al.* (JLQCD Collaboration), Phys. Rev. D **77**, 074503 (2008).
- [16] S. Aoki *et al.* (JLQCD Collaboration) (to be published).
- [17] T. Kaneko *et al.* (JLQCD Collaboration), Proc. Sci., LAT2007 (2007) 148 [arXiv:0710.2390].
- [18] S. Hashimoto *et al.* (JLQCD Collaboration), Proc. Sci., LAT2007 (2007) 101 [arXiv:0710.2730].